J. Cell. Mol. Med. Vol 16, No 3, 2012 pp. 507-519

Relaxin promotes growth and maturation of mouse neonatal cardiomyocytes *in vitro*: clues for cardiac regeneration

Silvia Nistri [a, #], Alessandro Pini [a, #], Chiara Sassoli [b], Roberta Squecco [c], Fabio Francini [c], Lucia Formigli [b], Daniele Bani [a, *]

[a] *Department of Anatomy, Histology & Forensic Medicine, Section Histology, University of Florence, Florence, Italy*
[b] *Department of Anatomy, Histology & Forensic Medicine, Section Anatomy, University of Florence, Florence, Italy*
[c] *Department of Physiological Sciences, University of Florence, Florence, Italy*

Received: March 25, 2011; Accepted: April 11, 2011

Abstract

The demonstration that the adult heart contains myocardial progenitor cells which can be recruited in an attempt to replace the injured myocardium has sparkled interest towards novel molecules capable of improving the differentiation of these cells. In this context, the peptide hormone relaxin (RLX), recently validated as a cardiovascular hormone, is a promising candidate. This study was designed to test the hypothesis that RLX may promote the growth and maturation of mouse neonatal immature cardiomyocytes in primary culture. The cultures were studied at 2, 12, 24 and 48 hrs after the addition of human recombinant H2 RLX (100 ng/ml), the main circulating form of the hormone, or plain medium by combining molecular biology, morphology and electrophysiology. RLX modulated cell proliferation, promoting it at 2 and 12 hrs and inhibiting it at 24 hrs; RLX also induced the expression of both cardiac-specific transcription factors (GATA-4 and Nkx2-5) and cardiac-specific structural genes (connexin 43, troponin T and HCN4 ion channel) at both the mRNA and protein level. Consistently, RLX induced the appearance of ultrastructural and electrophysiological signs of functionally competent, mature cardiomyocytes. In conclusion, this study provides novel circumstantial evidence that RLX specifically acts on immature cardiomyocytes by promoting their proliferation and maturation. This notion suggests that RLX, for which the heart is both a source and target organ, may be an endogenous regulator of cardiac morphogenesis during pre-natal life and could participate in heart regeneration and repair, both as endogenous myocardium-derived factor and exogenous cardiotropic drug, during adult life.

Keywords: relaxin • cardiomyocytes • proliferation • maturation

Introduction

Ischaemic heart disease and related cardiac failure affect an ever-increasing number of participants, depending on the ageing of population and elongation of life expectation, with a mean 5-year survival of 50–70% [1]. This is the main reason for the interest in the development of new therapeutic strategies aimed to regenerate, at least in part, the injured myocardium and to prevent or delay the progression of cardiac failure. Until recently, the myocardium has been considered a terminally differentiated tissue, without self-renewal potential. Therefore, attempts to replace the demised cardiomyocytes have been mainly based on the administration of exogenous stem cells, relying on their ability to settle into the diseased host myocardium and to differentiate into the cellular constituents of the heart. However, concerns remain as to whether these approaches can provide enough new myocyte mass to restore the mechanical function of the heart [2]. The recent demonstration that the adult heart contains a pool of cardiac stem cells [3,4], both in normal and pathological conditions, has dramatically changed the traditional view of the heart as a post-mitotic organ. The identification of spontaneous myocardial regeneration after ischaemic injury [3,5] indicates that endogenous cardiac progenitor cells, located in the viable myocardium

[#]These authors contributed equally to this paper.
*Correspondence to: Prof. Daniele BANI, M.D.,
Department of Anatomy, Histology & Forensic Medicine,
Section of Histology, University of Florence,
viale G. Pieraccini 6, I-50139 Florence, Italy.
Tel.: +39 055 4271 390
Fax: +39 055 4271 385
E-mail: daniele.bani@unifi.it

doi:10.1111/j.1582-4934.2011.01328.x

surrounding the infarcted area, can be recruited in an attempt to replace the dead myocardium. However, this phenomenon is not functionally relevant, conceivably because the myocardial progenitors in the adult heart have an intrinsically low regenerative potential and are operating in an unfavourable environment, as that occurring in the post-infracted myocardium [6]. In principle, the persistence of a pool of cardiac stem cells in the adult heart provides the background for possible therapeutic approaches alternative to exogenous stem cell transplantation [7]. Therefore, studies aimed at testing molecules potentially capable of improving the recruitment, self-renewal and *in situ* differentiation of resident cardiac progenitors are topical and clinically relevant. In this context, the peptide hormone relaxin (RLX) emerges as a promising candidate. RLX, best known for its effects on reproduction [8], has been recently validated as a cardiovascular hormone [9–12]. In fact, RLX is produced by cardiomyocytes [13–15] and binds to specific myocardial receptors [13,16–18]. On these grounds, RLX was hypothesized to play a role in cardiac development during intrauterine and neonatal life [13]. Of interest, human recombinant RLX has been recently proven an useful drug in patients with acute cardiac failure, as it was capable of improving key parameters of circulatory dysfunction [19–21]. The mechanisms underlying the functional improvement remain obscure, but conceivably are diverse and include the ability of RLX to exert direct inotropic effects, improve blood supply and decrease ventricular stiffness due to improved myocardial remodelling [12].

Based on the above considerations, in this study we aimed at extending the current knowledge on the cardiotropic effects of RLX by investigating the intriguing hypothesis that this hormone could also influence the growth and maturation of resident myocardial progenitor cells. To test this hypothesis, we used an *in vitro* model of immature cardiomyocytes isolated from neonatal mouse hearts [22], whose *in vitro* pattern of maturation has been well characterized in our previous studies [23].

Materials and methods

Cell culture

Primary cultures of mouse ventricular immature cardiomyocytes were prepared from hearts of 1-day old newborn CD1 albino mice (Harlan, Correzzana, Italy) following the protocol used for the cardiac beating assay [22], with minor modifications [23]. This is a well-established method to obtain myocardium-specific cell cultures, similar to the so-called cardiospheres, which are well-suited for functional studies. Briefly, hearts were quickly excised, the atria were cut-off and the ventricles minced and digested at 37°C for 45 min. in calcium-free HEPES-buffered Hanks' solution, pH 7.4, containing 100 μg/ml type II collagenase and 1X pancreatin (Invitrogen, Carlsbad, CA, USA). To reduce the harvest of non-myocardial cells, the tissue lysate was filtered through a 70 μm cell strainer (Millipore, Billerica, MA, USA) and pre-plated for 1 hr. The myocyte-enriched cells remaining in suspension were plated on glass cover slips placed in 35-mm tissue culture dishes for the confocal microscopy studies, or multi-well plates for the other experimental purposes. Culture supports were pre-coated with 1.5% gelatin for 30 min. Cardiomyocytes were cultured in DMEM containing 10% horse serum, 5% foetal bovine serum, and 1× gentamycin (Roche Molecular Biochemicals, Indianapolis, IN, USA). By this procedure, the cultures are composed of approx. 96% cardiomyocytes, as judged by vimentin immunofluorescence staining to identify residual fibroblasts, coronary endothelial and endocardial cells [23]. Moreover, these cells have been shown to express the specific RLX receptor RXFP1 [23]. Twelve hours after plating, the culture medium was changed and added with human recombinant H2 RLX, the main circulating form in human beings [8], kindly provided by Prof. Mario Bigazzi (Foundation for the Study of Relaxin in Cardiovascular and Other Diseases, Prosperius Institute, Florence, Italy), at the concentration of 100 ng/ml. This dose was selected as it was found to have marked biological effects in previous studies on isolated mouse cardiomyocytes [24] as well as in models of cardiac ischaemia-reperfusion *in vitro* and *in vivo* in different animal species [25,26]. The cultures were studied at 2, 12, 24 and 48 hrs after the RLX addition. Control cardiomyocyte cultures, not treated with RLX, were also studied at the same time points.

Cell proliferation analysis by ^{3}H-thymidine incorporation

To evaluate whether RLX affected cell proliferation, freshly isolated cells were seeded in 24-well plates, approximately 10^{4} cells/well, and cultured for 2, 12, 24 and 48 hrs in DMEM in the absence or presence of RLX (100 ng/ml). After the incubation, the medium was replaced with Hank's Balanced Salt Solution (HBSS; Gibco-Invitrogen, S.Giuliano Milanese, Italy) containing 18.5 kBq/ml (0.5 μCi/ml) ^{3}H-thymidine for 1 hr at 37° C. The medium was then removed, the cultures washed with plain HBSS and DNA precipitated with cold 3% TCA and extracted with 1 ml of 0.3M NaOH. The recovered radioactivity was measured in a β counter (1900 TR; Packard, Zurich, Switzerland). The experiments were performed in triplicate and the values expressed as dpm/mg of proteins, the latter measured with the bicinchoninic acid (BCA) assay (mean ± S.E.M.).

Based on these results, ^{3}H-thymidine incorporation by cardiomyocytes in the earlier phases of active growth was also investigated by histoautoradiography. Briefly, cardiomyocytes seeded onto glass slides were grown for 2 and 12 hrs in DMEM in the absence or presence of RLX (100 ng/ml). After the incubation, the medium was replaced with (HBSS; Gibco-Invitrogen) containing 37 kBq/ml (1 μCi/ml) ^{3}H-thymidine for 1 hr at 37° C. Then, the cells were fixed in Carnoy's fixative for 20 min., the slides were washed overnight in distilled water, dipped in photographic emulsion (K5; Ilford Photo, Mobberley, UK) at 50°C, dried at 20°C, and exposed in the dark for 7 days at 4°C. After exposure, the slides were immersed in D19 developer (1:1 in distilled water; Kodak Ltd., Milan, Italy) for 8 min. at 20°C. Development was stopped by immersion in 1 M acetic acid for 2 min at 20°C and the slides were fixed for 6 min. at 20°C in Amfix (1:5 in distilled water; May and Baker, Eccles, UK), rinsed for 1 hr in distilled water, counterstained with haematoxylin, dehydrated and mounted in Eukitt medium. The percentage of labelled cells over total cells was calculated on 10 randomly chosen microscopical fields viewed with a 40× objective by a trained observer who was unaware as to the experimental group of the autoradiographic slides he was scoring.

RNA isolation

Total RNA was isolated by extraction with TRIzol Reagent (Invitrogen Life Technologies, Grand Island, NY, USA), according with the manufacturer's

instructions. Potential contaminating DNA was removed with DNase (Deoxiribonuclease I; Sigma-Aldrich, Milan, Italy) prior to the reverse transcription (RT) reaction. Concentration and purity of extracted RNA were evaluated prior and after the DNase treatment by spectrophotometry, by measuring the absorbance at 260 and 280 nm wavelength. The absence of RNA degradation was confirmed by agarose gel electrophoresis with ethidium bromide staining.

Real-time PCR

One microgram of total RNA was reverse transcribed to single-stranded cDNA using the commercially available i-script cDNA Synthesis Kit (BioRad, Foster City, CA, USA), according to the manufacturer's instructions. Samples were incubated at 25°C for 5 min., at 42°C for 30 min. and then at 85°C for 5 min. in a thermal cycler. Negative controls of the RT were performed by omitting the enzyme or by substituting the RNA for sterile RNAse-free water, to control for genomic DNA and RNA contamination, respectively. Quantitative real-time PCR was carried out using the ABI Prism 7500 Sequence Detection System instrumentation (Applied Biosystems, Carlsbad, CA, USA) and Taqman gene expression assay reagents (Applied Biosystems), consisting in a specific set of primers and a fluorogenic internal probe. The expression of five-key target genes involved in cardiomyocyte differentiation was quantitated in comparison with the housekeeping gene GAPDH (Table 1). PCR amplifications were performed in Optical 96-well plates (Applied Biosystems) on cDNA samples corresponding to a final RNA concentration of 50 ng. PCR was performed in a total volume of 20 μl containing 2× Taqman Universal PCR Master mix (Applied Biosystems) and 20× Taqman gene expression assays. Reaction conditions were as follows: 50°C for 2 min., 95°C for 10 min., followed by 40 cycles at 95°C for 15 s alternating with 60°C for 1 min. PCR amplifications were run in triplicate. Blank controls, consisting in no template (water) or RT-negative reactions, were performed in each run. The results of the real-time PCR data were represented as Ct values, where Ct was defined as the PCR threshold cycle at which amplified product was first detected. Ct values were analysed using $2^{-\Delta\Delta Ct}$ method. All values were normalized to the GAPDH housekeeping gene expression (Table 1).

Table 1 Genes analysed by real-time PCR

Gene	Function	TaqMan gene expression code
GATA-4*	Cardiac myogenic transcription factor [29]	Mm00484689_m1
Nkx2-5*	Cardiac myogenic transcription factor [28]	Mm00657783_m1
Cx43*	Cardiac gap junctional protein [30,31]	Mm00439105_m1
CTnT*	Cardiac sarcomeric protein	Mm00441922_m1
HCN4*	K^+ channel involved in cardiac pace making [32]	Mm01176086_m1
GAPDH†	Carbohydrate metabolism enzyme	Mm99999915_g1

*Target genes. †Housekeeping gene.

Confocal immunofluorescence microscopy

Paraformaldehyde-fixed cells grown onto glass cover slips were immunostained with the following primary antibodies: goat polyclonal anti–GATA-4 (1:50; Santa Cruz Biotechnology, Santa Cruz, CA, USA); mouse monoclonal anti-connexin 43 (Cx43, 1:200; Chemicon, Temecula, CA, USA); mouse monoclonal anti-cardiac troponin T (cTnT, 1:100; LabVision, Fremont, CA, USA); rabbit polyclonal anti-hyperpolarization– activated cyclic nucleotide-gated channel HCN4 (1:100; Santa Cruz). Immune reaction was revealed using the appropriate Alexa-conjugated secondary antibodies (1:100; Molecular Probes, Eugene, OR, USA). Negative controls were performed by replacing the primary antisera with corresponding non-immune sera from the same animal species. Cells were examined with a Leica TCS SP5 confocal laser scanning microscope (Leica Microsystem, Mannheim, Germany) equipped with a Leika PlanApo 63× oil-immersion objective and a HeNe/Argon laser source for fluorescence measurements and with differential interference contrast (DIC) optics for transmission images. A series of optical sections (1024 × 1024 pixels) at intervals of 0.8 μm were obtained and superimposed to create a single composite image. Densitometric analysis of the intensity of the immunofluorescent staining for the assayed markers was performed on digitized images of the cultures using the free-share ImageJ software (http://rsbweb.nih.gov/ij). Briefly, a test area of 100 μm^2 was used to measure 5 volumes of interest, 6 μm thick, in each confocal stack. Five confocal stacks were selected at random for each experimental condition. The mean ± S.E.M. optical density was then calculated.

Transmission electron microscopy

Cardiomyocytes grown for 48 hrs in the presence or absence of RLX (100 ng/ml) were pelleted by centrifugation, fixed in 4% glutaraldehyde, post-fixed in 1% osmium tetroxide and embedded in Epon 812. Ultrathin sections were stained with uranyl acetate and alkaline bismuth subnitrate and examined under a JEM 1010 electron microscope (Jeol, Tokyo, Japan) at 80 kV.

Electrophysiology

The electrophysiological features of cardiomyocytes were investigated by whole-cell patch-clamp, as described [23, 24], at 24 and 48 hrs. In particular, we evaluated: (i) occurrence of rhythmic action potentials (APs); (ii) inward Na^+ current, $I_{Na,}$; (iii) T-type ($I_{Ca,T}$) and L-type ($I_{Ca,L}$) Ca^{2+} currents; (iv) depolarization-activated transient outwards K^+ current I_{to}; (v) the inward rectifier I_{K1}; (vi) the pacemaker current I_f. The patch-clamp assay was performed using micromanipulator-operated micropipettes connected to an Axopatch 200B amplifier (Axon Instruments, Molecular Devices, Sunnyvale, CA, USA). Cells to be analysed were selected among the smallest cell clusters (max. five cells). Both voltage-clamp and current-clamp modes were used. Whole-cell recording was established in the voltage-clamp mode and compensation for the pipette capacitance was performed before switching into the current-clamp mode to record the AP of spontaneously beating cells. In our experimental protocol, cells were allowed to grow for 24 and 48 hrs and establish physiological cell–cell contacts and gap junctional communications, which are required for cardiomyocyte maturation. Just before performing the recordings, heptanol (1 mM) was added to block gap junctional communication. In this way, the cells were

only uncoupled during the electrophysiological experiments. Protocol generation and data acquisition were controlled by using two output and input of the A/D-D/A interfaces (Axon Digidata 1200; Molecular Devices) and Axon Pclamp 9 software (Molecular Devices). Unless otherwise stated, the used reagents were from Sigma-Aldrich. The experiments were carried out in normal Tyrode (NT) bath solution of the following composition (mM): NaCl 140, KCl 5.4, $CaCl_2$ 1.5, $MgCl_2$ 1.2, glucose 5.5, HEPES/NaOH 5, at room temperature. The choice to perform the experiments at a temperature below the physiological 37°C aimed at extending the life span of the cells during the experiments, as well as improving the recording of the details of current traces, particularly the fastest currents. To test high-voltage–activated Na^+ channel sensitivity, we used tetrodotoxin (TTX, 1 μM). When outward K^+ currents had to be suppressed, experiments were performed in 20 mM tetraethylammonium (TEA) bath solution composed by (mM): 122.5 NaCl, 2 $CaCl_2$, 20 TEA-OH, 10 HEPES. The K^+ channel blocker 4-aminopyridine (2 mM) was also used to test for the occurrence of 4-aminopyridine–sensitive transient outward K^+ current, I_{to}. Ca^{2+} currents were recorded in Na^+-and K^+-free TEA-Ca^{2+} bath solution containing (mM): 10 $CaCl_2$, 145 TEA bromide, 10 HEPES. In turn, 10 μM nifedipine were added to block L-type Ca^{2+} channels. To record I_{K1} or I_f, 4 mM Cs^+ or 0.5 mM Ba^{2+} was applied to the bath solution [27]. The pH of the bath solution was adjusted to 7.4 with NaOH. Patch pipette filling sterile solution contained (mM): 130 KCl, 10 NaH_2PO_4, 0.2 $CaCl_2$, 1 EGTA, 5 MgATP, 10 HEPES, adjusting pH to 7.2 with KOH. The rapid inward Na^+ (I_{Na}) and Ca^{2+} currents were evoked by 1 sec. voltage pulses ranging from −80 to +50 mV in 10 mV increments applied from a holding potential (HP) of −90 mV. The K^+ current ($I_{K,tot}$) flowing through delayed rectifier channels was elicited in voltage clamp conditions from an HP of −60 mV to block Na^+ current (I_{Na}) and T-type Ca^{2+} current ($I_{Ca,T}$) and in the presence of nifedipine to block L-type Ca^{2+} current ($I_{Ca,L}$). Pulse stimulation protocol consisted of voltage steps in 10 mV increments ranging from −80 to +50 mV. The I_{to} was elicited by 1 sec. voltage steps from −40 to +50 mV applied from an HP of −60 mV, being I_{Na} and T-type Ca^{2+} current inactivated. The inward rectifier current (I_{K1}) was evoked by ramp voltage-clamp pulses applied from an HP of −120 to +40 mV at a rate of 100 mV/sec. The I_f pacemaker current was evoked by hyperpolarizing steps ranging from −30 to −150 mV in 20-mV increments applied from a HP of −30 mV. APs were recorded by switching the amplifier to current clamp mode. The passive membrane capacitance C_m was used as an index of the membrane surface area, considering the specific value of 1 μF/cm^2. In this way, as C_m ranged between 58 and 118 pF in the different experimental conditions (Table 2, first line), the calculated surface area varied from 58 to 118 10^{-6} cm^2. Data are reported as current density (I/C_m) and specific conductance (G/C_m) to allow comparison of test currents recorded from different cells. The steady-state ionic current of activation was evaluated by the formula: $I_a(V) = G_{max}(V - V_{rev})/\{1 + \exp[(V_a - V)/k_a]\}$ and steady-state inactivation of I_f by the formula: $I_h(V) = I/\{1 + \exp[-(V_h - V)/k_h]\}$, where G_{max} is the maximal conductance for the I_a, V_{rev}, is the apparent reversal potential, V_a and V_h are the potentials that elicit, respectively, the half-maximal activation and inactivation values, k_a and k_h are the steepness factors.

Statistical analysis

Statistical analysis of differences between the control and the RLX-treated cultures at the assayed time points was performed using one-way ANOVA and *post hoc* test. The differences between paired values of the real-time PCR assay were analysed by Student's *t*-test. Calculations were performed using the GraphPad Prism 4.0 statistical software (GraphPad, San Diego, CA, USA).

Results

The cultured cardiomyocytes were examined at different time points (2, 12, 24 and 48 hrs) from the addition of culture medium in the presence or absence of RLX by phase-contrast light microscopy (data not shown). At the earliest time, they appeared as scattered round- or polyhedral-shaped cells with no spontaneous beating, consistent with their nature of immature cardiomyocytes. From 12 hrs onwards, the isolated cells spontaneously tended to gather into aggregates which contracted rhythmically and became larger with time, as previously reported [23]. RLX did not appear to induce major morphological changes of the overall appearance of the cultures, apart from a larger size of the cardiomyocyte aggregates and an increased number of the stripe-like cells at the later time points. These effects of RLX were conceivably ascribable to its ability to stimulate cell proliferation in the short term. In fact, as revealed by ^{3}H-thymidine incorporation (Fig. 1A and B), RLX significantly increased the amount of cycling cells at the earlier time points, especially upon the 12-hr incubation. On the other hand, at 24 hrs, RLX significantly reduced the amount of cycling cells, whereas it did not induce appreciable changes at 48 hrs. Histoautoradiography (Fig. 1B) confirmed that RLX, at the earlier time points, markedly stimulated cell proliferation: in fact, the percentage of cycling cells was significantly increased at 2 hrs (5.4 ± 1.1 *versus* 2.3 ± 0.6 in the controls, $n = 10$, $P < 0.02$ by Student's *t*-test) and even higher at 12 hrs (7.4 ± 1.2 *versus* 1.7 ± 0.4 in the controls, $n = 10$, $P < 0.001$ by Student's *t*-test).

The real-time PCR analysis revealed that RLX up-regulated the expression of key genes involved in myocardial differentiation (Fig. 2). In particular, as compared with the control cultures, the transcripts for myogenic transcription factors GATA-4 and Nkx2-5, which are required to induce the expression of cardiac-specific structural genes during cardiomyocyte maturation [28,29], were significantly increased by RLX by the 24- and 48-hrs time points, with an overt inverse relationship with cell growth stimulation. Consistent with these findings, the transcript for Cx43, which is crucial for the intercellular coupling and transmission of the electrical excitation among cardiomyocytes [30,31], was significantly enhanced by RLX starting from 24 hrs onwards. Moreover, the mRNA levels of cTnT, a typical sarcomeric protein, was also increased by RLX, reaching a maximum at 48 hrs. Finally, the transcript for HCN4, a hyperpolarization-activated cyclic nucleotide-gated mixed Na^+/K^+ channel involved in cardiac pace-making I_f current [32] was also affected by RLX, showing significantly increased expression at any time point assayed, with a peak at 24 hrs.

In keeping with the above findings, the immunofluorescence analysis revealed that RLX enhanced the expression of representative differentiation proteins, including GATA-4, Cx43, cTnT and HCN4 (Fig. 3). In particular, GATA-4 was expressed in both the cytoplasms and the nuclei, consistently with its synthesis and subsequent translocation into the nucleus. Densitometric quantification of the immunostaining showed that, upon a 2-hr incubation,

Table 2 Membrane capacitance (C_m) and activation Boltzmann parameters of I_{Na}, $I_{Ca,T}$, $I_{Ca,L}$ and I_f currents in the cardiomyocytes grown for 24 and 48 hrs in the absence or the presence of RLX

Currents	Parameters	−RLX (24 hrs)	+RLX (24 hrs)	−RLX (48 hrs)	+RLX (48 hrs)
	C_m (pF)	58 ± 5	75 ± 8**	95±8 §§§	118 ± 12** §§§
I_{Na}	I_p (pA/pF)	325 ± 30	500 ± 55**	400±42§§	620 ± 61** §§§
	G_m (nS/pF)	4.5 ± 0.3	8.1 ± 0.6 **	5.1±0.4 §	9.8 ± 0.9** §§
	V_a (mV)	−26.1 ± 2.1	−27.2 ± 2.8	−27.5±2.7	−30.3 ± 3.1* §
	K_a (mV)	6.4 ± 0.4	6.2 ± 0.4 *	6.2 ± 0.4	5.7 ± 0.4* §
	V_r (mV)	47.4 ± 4	47.0 ± 4	48.6 ± 4	47.1 ± 5
$I_{Ca,T}$	I_p (pA/pF)	2.0 ± 0.2	2.9±0.3***	2.4 ± 0.2 §	3.5 ± 0.3*** §§
	G_m (pS/pF)	20.1 ± 2.1	30.1 ± 2.4 **	20.3 ± 2.1	40.2 ± 3.3*** §§
	V_a (mV)	−37.0 ± 3.6	−36.7± 3.8	−36.5±3.2	−37.2 ± 4.2
	K_a (mV)	7.1 ± 0.5	6.9± 0.5	6.9±0.5	6.6 ± 0.5
	V_r (mV)	68.4 ± 5	67.1 ± 4 ±	69.1 ± 4	67.7 ± 4
$I_{Ca,L}$	I_p (pA/pF)	8.1 ± 0.8	16 ± 1.2**	11±0.9 §§	25±1.6** §§§
	G_m (pS/pF)	100 ± 10.3	159.7 ± 15.5 **	150.2 ± 12.2§§§	251.3 ± 20.2*** §§§
	V_a (mV)	−11.8 ± 1.1	−13.2 ± 1.2	−13.2±1.2 §	−14.6 ± 1.2* §
	K_a (mV)	7.5 ± 0.6	6.9 ± 0.5 *	7.1 ± 0.6	5.9 ± 0.5** §§
	V_r (mV)	69.4 ± 5	67.4 ± 4	68.1 ± 4	69.1 ± 4
I_{to}	$I_{to,50}$ (pA/pF)	5.6 ± 0.5	8.3 ± 0.7**	7.1 ± 0.6 §§	11 ± 0.9** §§
I_{K1}	$I_{K1,-120}$ (pA/pF)	7.5 ± 0.6	9.5 ± 0.8**	11.4±0.9 §§	13.5 ± 1.1** §§§
I_f	$I_{f,-150}$ (pA/pF)	5.0 ± 0.3	5.5 ± 0.3*	6.8±0.5 §§	8.1 ± 0.6** §§§
	G_m (pS/pF)	33.6 ± 3.5	38.5 ± 4.2 *	46.2 ± 3.8 §§	55.4 ± 4.4** §§§
	V_a (mV)	−93.1 ± 9.3	−92.2 ± 9.4	−92.2 ± 8.4	−92.2 ± 8.4
	K_a (mV)	16.4 ± 0.3	16.1 ± 0.4	16.1 ± 0.4	15.6 ± 0.4

I_p: data of the peak current at the voltage eliciting the maximal current; I_{to}: data at 50 mV; I_{K1}: data at −120 mV; I_f: data at −150 mV; $I_{Ca,T}$ evaluated in the presence of nifedipine, and $I_{Ca,L}$ evaluated after detracting $I_{Ca,T}$ from the total Ca^{2+} current ($I_{Ca,tot}$, see also Fig. 7D). Significance of differences (one-way ANOVA): −RLX *versus* +RLX, $*P < 0.05$, $**P < 0.01$, $***P < 0.001$; 24 hrs *versus* 48 hrs, $^{§}P < 0.05$, $^{§§}P < 0.01$, $^{§§§}P < 0.001$. Data are mean ± S.E.M. of the values from 26 to 35 cardiomyocytes.

there were no appreciable differences between the control and the RLX-treated cultures, whereas marked, statistically significant increase in the immunoreactivity for the noted proteins was detected upon a 48-hr incubation with RLX (Fig. 3).

The ultrastructural analysis confirmed that RLX promotes cardiomyocyte maturation. In fact, the cardiomyocytes grown for 48 hrs in the absence of RLX mostly showed an organellular complement typical of immature cells, containing free polyribosomes, some dilated rough endoplasmic reticulum (RER) cisternae, diffuse cytoskeletal components, sparse glycogenic fields and small, round-shaped mitochondria (Fig. 4A). Instead, at the same end-point, the RLX-treated cardiomyocytes mostly displayed muscle cell features, with numerous leptomeres, that is cross-banded structures composed of periodically arranged electron-dense bands bridged by 5-nm-thick filaments [33], and abundant mitochondria with packed cristae and condensed matrix (Fig. 4B). Cells at a more advanced stage of striated muscle maturation, containing myofibrillar structures, rod-shaped mitochondria with electron-dense matrix granules and intercellular junctions featuring rudimentary intercalated discs were seldom encountered in the RLX-treated cultures, but not in the control ones (Fig. 4C).

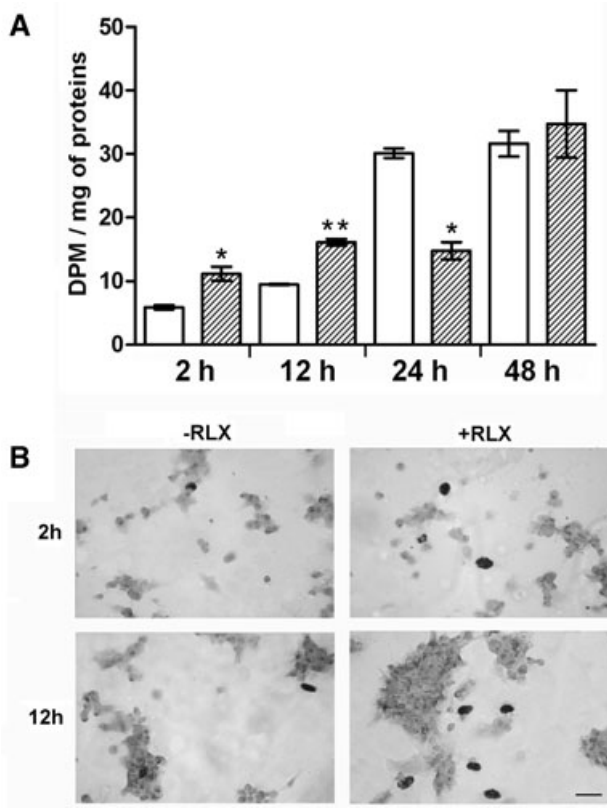

Fig. 1 Cell proliferation analysed at the noted time points from the addition of fresh culture medium, alone (open columns) or with RLX added (striped columns): (**A**) ^{3}H-thymidine incorporation and β-counting (DPM: disintegrations per minute); (**B**) histoautoradiography of ^{3}H-thymidine–labelled cardiomyocytes. RLX significantly increases the number of cycling cells at 2 and 12 hrs. On the other hand, the cells' growth rate decreases at 24 hrs in comparison with the control cultures and remains unchanged at 48 hrs. Significance of differences (one-way ANOVA, $n = 3$): $^{*}P < 0.05$; $^{**}P < 0.01$. Bar (lower right) = 20 μm.

Once assessed that RLX, at 24 and 48 hrs, was capable of prompting the cardiomyocytes towards a biochemically mature phenotype, we next investigated by electrophysiology, at the same time points, whether these cells would also acquire a functional electrical phenotype. By whole-cell patch in current clamp mode, the control cardiomyocytes, assayed at 24 hrs, showed spontaneous rhythmic APs with a slow depolarization phase 4 (pacemaker current) from a maximal diastolic potential (MDP) of -61.2 ± 5 to a voltage threshold for AP of -46.0 ± 5 mV [Figure 5A(a)]. When recording the membrane currents by voltage

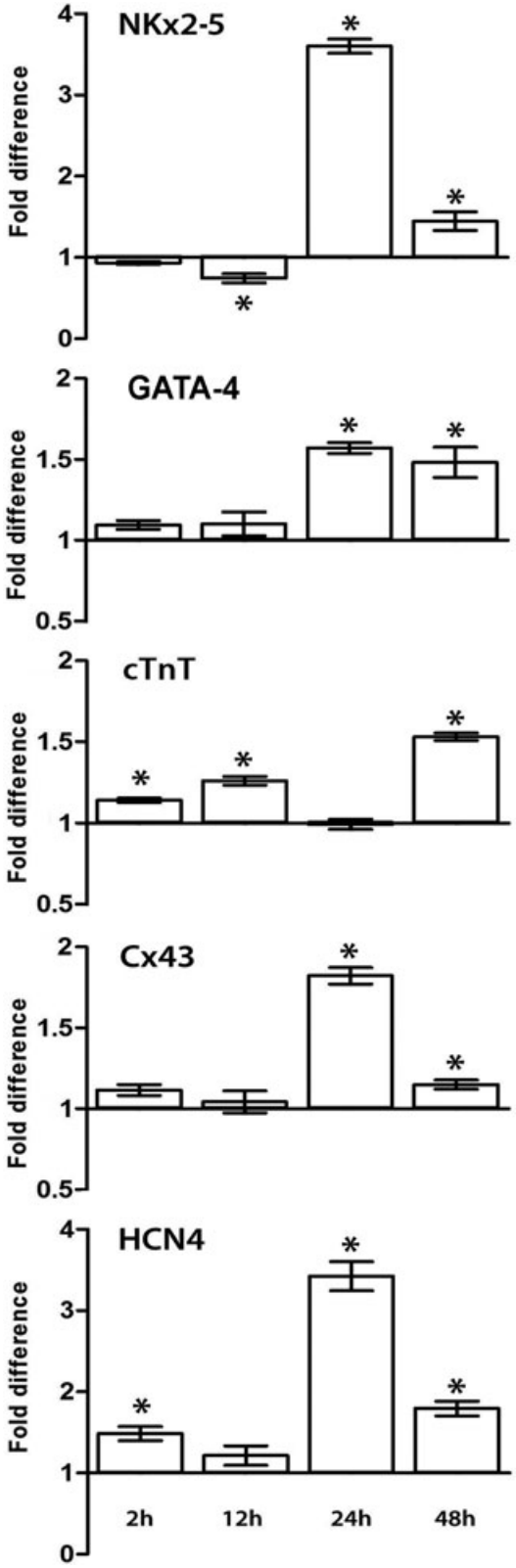

Fig. 2 Quantitative real-time PCR analysis showing the effects of RLX on the expression of mRNAs for the noted myocardial markers at the different time points. The columns represent fold changes over the corresponding values of the control cultures, assumed as 1. Significance of differences (Student's *t*-test, $n = 3$): $^{*}P < 0.05$ *versus* the controls.

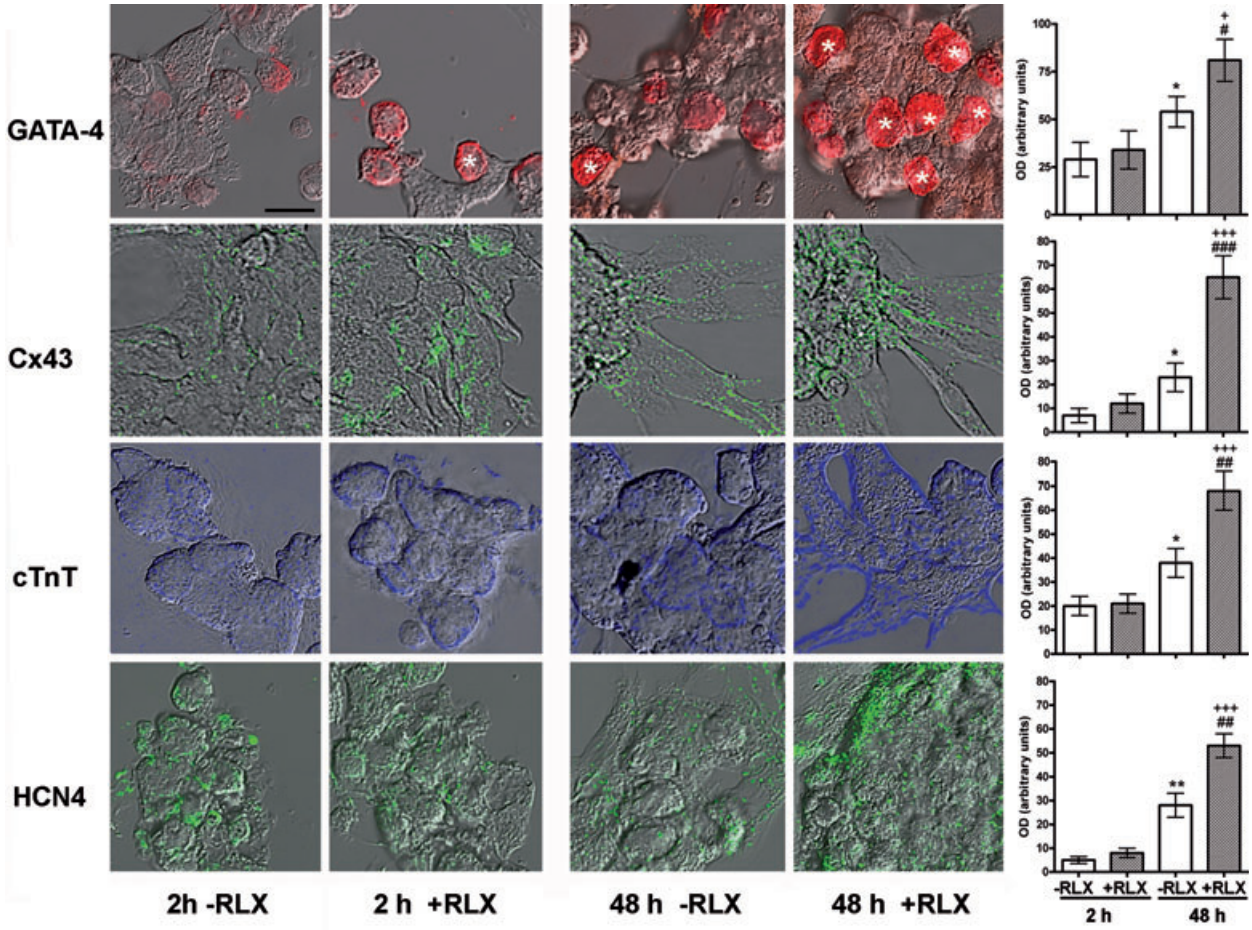

Fig. 3 Representative merged differential interference contrast and confocal immunofluorescent micrographs of cardiomyocytes cultured for 2 and 48 hrs in the absence or presence of RLX. Immunoreactivities for the different antigens are shown in pseudo-colours. There is a visible increase in the immunoreactivity for the noted antigens upon a 48-hrs incubation with RLX. GATA-4–positive nuclei are indicated by asterisks. Bar (upper left) = 16 μm. The right panels show the computer-aided densitometry of the immunostaining for the noted myocardial marker proteins. Significance of differences (one-way ANOVA, $n = 5$): $^{*}P < 0.05$ and $^{**}P < 0.01$ *versus* −RLX 2 hrs; $^{+}P < 0.05$ and $^{+++}P < 0.001$ *versus* +RLX 2 hrs; $^{\#}P < 0.05$, $^{\#\#}P < 0.01$ and $^{\#\#\#}P < 0.01$ *versus* −RLX 48 hrs.

clamp to elucidate the ionic basis for AP dynamics (Fig. 5B–D), the cardiomyocytes showed: (i) a prominent inward Na^+ current, I_{Na}, in the first 3–4 msec. of the pulse starting from a threshold of −49.5 ± 4 mV, blocked by TTX (Fig. 5B and D); (ii) two Ca^{2+} currents which, based on voltage dependence and nifedipine sensitivity, were identified as the transient T-type ($I_{Ca,T}$) and L-type ($I_{Ca,L}$) Ca^{2+} currents: $I_{Ca,T}$ was evoked from −60 mV, whereas $I_{Ca,L}$ was elicited from −30 mV with a slower activation and inactivation rate (Fig. 5C(a) and D); (iii) typical K^+ currents of mature cardiomyocytes [23], including fast transient outward I_{to} (Fig. 6A) blocked by 2 mM 4-aminopyridine, and inward rectifier I_{KI} recorded with external solution containing 3 mM Cs^+ (Fig. 6B); (iv) the pacemaker current I_f recorded in external solution containing 0.5 mM of Ba^{2+} [Fig. 6C(a–c)]. Despite the occurrence of I_f, which fits well with the expression of HCN4 channel, the cultured cardiomyocytes should not be identified as pacemaker cells: in fact, they did show a small early upstroke of the AP, which is lacking in authentic pacemaker cells because of defective or absent expression of Na channels. As expected, the cardiomyocytes underwent spontaneous time-dependent maturation, as judged by: (i) the amplitude of AP overshoot, which increased from 12 ± 3 mV (24 hrs) to 25 ± 3 mV (48 hrs; $P < 0.01$); (ii) AP duration quantified at 90% repolarization, which decreased from 128 ± 13 msec. (24 hrs) to 105 ± 10 msec. (48 hrs; $P < 0.05$); (iii) beating rate, which increased from 72 ± 9 (24 hrs) to 110 ± 15 beats/min. (48 hrs; $P < 0.01$). Moreover, at the later time point (48 hrs), the cardiomyocytes showed an increase in membrane capacitance (C_m), an indirect index of cell size (Table 2) I_{Na}, $I_{Ca,T}$ and $I_{Ca,L}$ current size and G_{Na}, $G_{Ca,T}$ and $G_{Ca,L}$ conductance (Fig. 5B–D, Table 2), and I_f, I_{to} and I_{KI} amplitudes (Fig. 6A–C, Table 2).

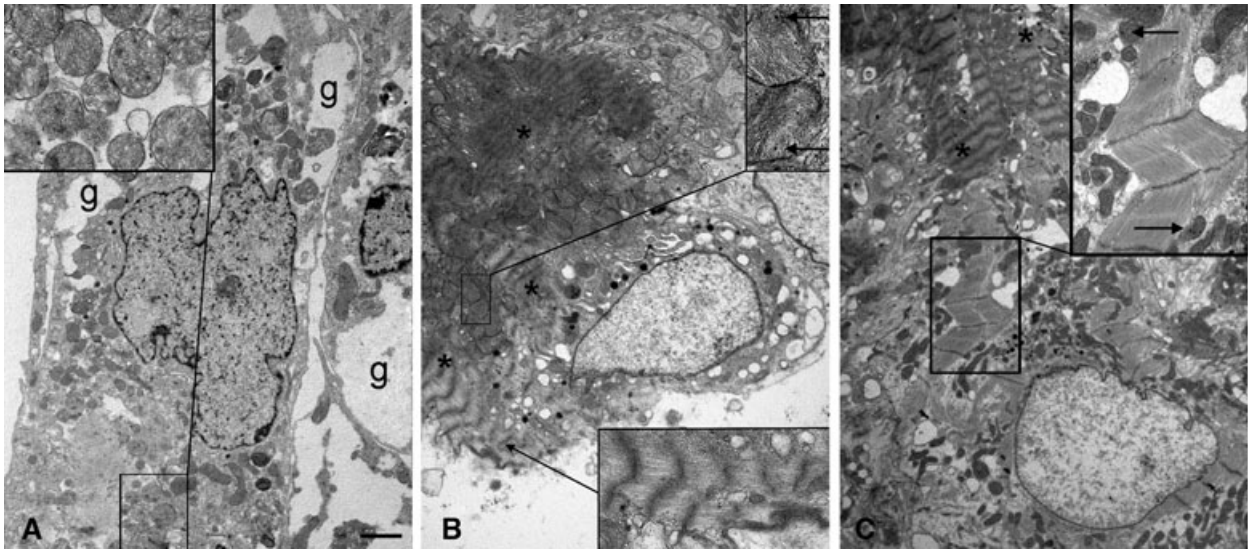

Fig. 4 Representative electron micrographs of cardiomyocytes cultured for 48 hrs in the absence (**A**) or presence of RLX (**B, C**). (**A**) An immature control cardiomyocyte showing round mitochondria (inset) and glycogen fields (g). (**B**) A more mature RLX-treated cardiomyocyte showing cytoplasmic leptomeres (asterisks, lower inset) and round mitochondria with densely stacked cristae and electron-dense matrix granules (upper inset, arrows). (**C**) Another mature RLX-treated cardiomyocyte showing myofibrils and rod-shaped mitochondria with electron-dense matrix granules (inset, arrows). The asterisks label the leptomeres in an adjacent cell. Bar (left) = 1 μm.

Of note, compared with the time-matched control cultures, the RLX-treated cardiomyocytes showed significantly higher values of the voltage-gated currents I_{Na}, $I_{Ca,T}$, $I_{Ca,L}$ and G_{Na}, $G_{Ca,T}$, $G_{Ca,L}$ conductance (Fig. 5B(b), C(b) and D; Table 2), I_f, I_{to} and I_{Kl} amplitude (Fig. 6A–C; Table 2) and significantly greater membrane capacitance, C_m (Table 2). Notably, RLX modified the voltage sensitivity of I_{Na} and $I_{Ca,L}$ currents because V_a values were shifted towards more negative potential, and K_a values were decreased. Finally, compared with the controls, the spontaneous firing rate of the RLX-treated cardiomyocytes increased to 120 ± 12 (24 hrs; $P < 0.01$) and 140 ± 14 beats/min. (48 hrs; $P < 0.01$; Fig. 5A b), in keeping with the reported chronotropic effects of the hormone [34]. Careful analysis of the reported electrophysiological findings supported the view that RLX can promote cardiomyocyte maturation towards the ventricular phenotype. In particular, this was suggested by: (i) the greater amplitude of the early upstroke of the AP (from 12 ± 3 to 32 ± 6 mV, $P < 0.01$ and from 25 ± 3 to 36 ± 6 mV, $P < 0.05$, at 24 and 48 hrs, respectively) and of AP itself (from 60 ± 5 to 80 ± 7 mV, $P < 0.01$ and from 70 ± 7 to 85 ± 7, $P < 0.05$, at 24 and 48 hrs, respectively) compared with the controls, confirmed by the greater G_m value of the Na current; (ii) the V_a features of T-type and L-type Ca^{2+} currents, whose values were more positive than those of typical atrial cardiomyocytes [35,36]; (iii) the increase of I_{K1} (Table 2, Fig. 6B), which was related to a significant decrease of AP duration quantified at 90% repolarization (24 hrs: 128 ± 13 *versus* 112.8 ± 10 with and without RLX, $P < 0.05$; 48 hrs: 105.1 ± 9 *versus* 98.2 ± 8 with and without RLX, $P < 0.05$) and to a more hyperpolarized MDP (24 hrs: −61.2 ± 5 *versus* −62.8 ± 5 with and without RLX; 48 hrs: −64.1 ± 5 *versus* −70.2 ± 5 with and without RLX, $P < 0.05$). I_{K1} and I_f exerted opposite effects on MDP and diastolic depolarization rate, in agreement with the counteracting roles of repolarizing I_{K1} and depolarizing I_f currents [27]. Hence, the size increase of I_f induced by RLX reduced in part the changes of MDP induced by I_{K1}. However, the role of I_{K1} on MDP prevailed on I_f, as the sizes of I_{K1} were 25–50% greater that those of I_f (Table 2).

Discussion

As in other organs provided with a stem cell pool, the normal heart is thought to harbour undifferentiated, quiescent cardiac stem cells (CSC), mainly located in epicardial 'cardiogenic niches' and characterized by low or null proliferative potential. Once recruited by appropriate stimuli, these cells may enter the cell cycle and give rise to immature cardiomyocytes, or cardiac precursors, characterized by higher proliferative potential and restricted commitment to the myocardial differentiation lineage [3,4]. Knowledge of the endocrine/paracrine factors controlling growth and differentiation of cardiomyocyte precursors is of pivotal interest to understand the physiological mechanisms involved in cardiac development, as well as to identify and validate new therapeutic strategies for the failing heart. In this context, the present *in vitro* study offers novel circumstantial evidence that the hormone RLX specifically acts on immature cardiomyocytes, which express the RLX receptor RXFP1 [23], by modulating proliferation and promoting maturation. This

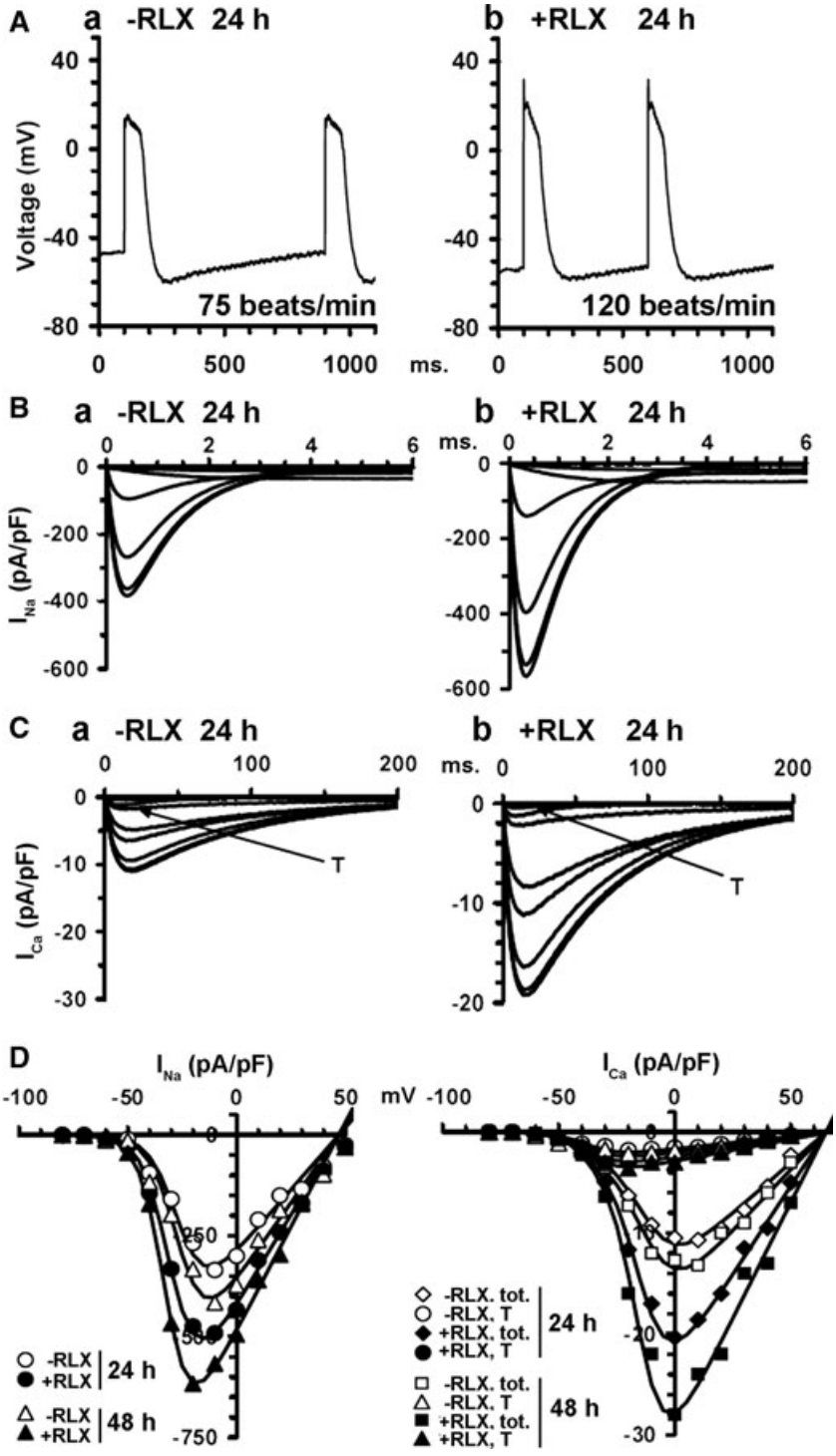

Fig. 5 Electrophysiological features of the neonatal cardiomyocytes cultured for 24 and 48 hrs in the absence (**a**) or presence of RLX (**b**). (**A**) Representative spontaneous action potentials recorded in current clamp mode at 24 hrs. (**B**) I_{Na} traces and (**C**) I_{Ca} traces recorded in voltage-clamp mode at 24 hrs: T indicates transient T-type I_{Ca}. (**D**) Boltzmann functions depicting *I–V* curves for I_{Na} peak, total $I_{Ca,tot}$ and T-type Ca^{2+} currents, recorded in the presence of nifedipine at 24 and 48 hrs. The related Boltzmann parameters and the statistical analysis are reported in Table 2. Data are mean values from 26 to 35 different cells.

notion suggests that RLX, for which the heart is both a source and target organ [9–12], may be an endogenous regulator of cardiac morphogenesis during pre-natal life, as previously suggested [13], and could participate in heart regeneration and repair during adult life, both as endogenous myocardium-derived factor and exogenous cardiotropic drug.

This study shows that RLX had a biphasic effect on cardiomyocyte growth, consisting in a stimulation at the earlier time points

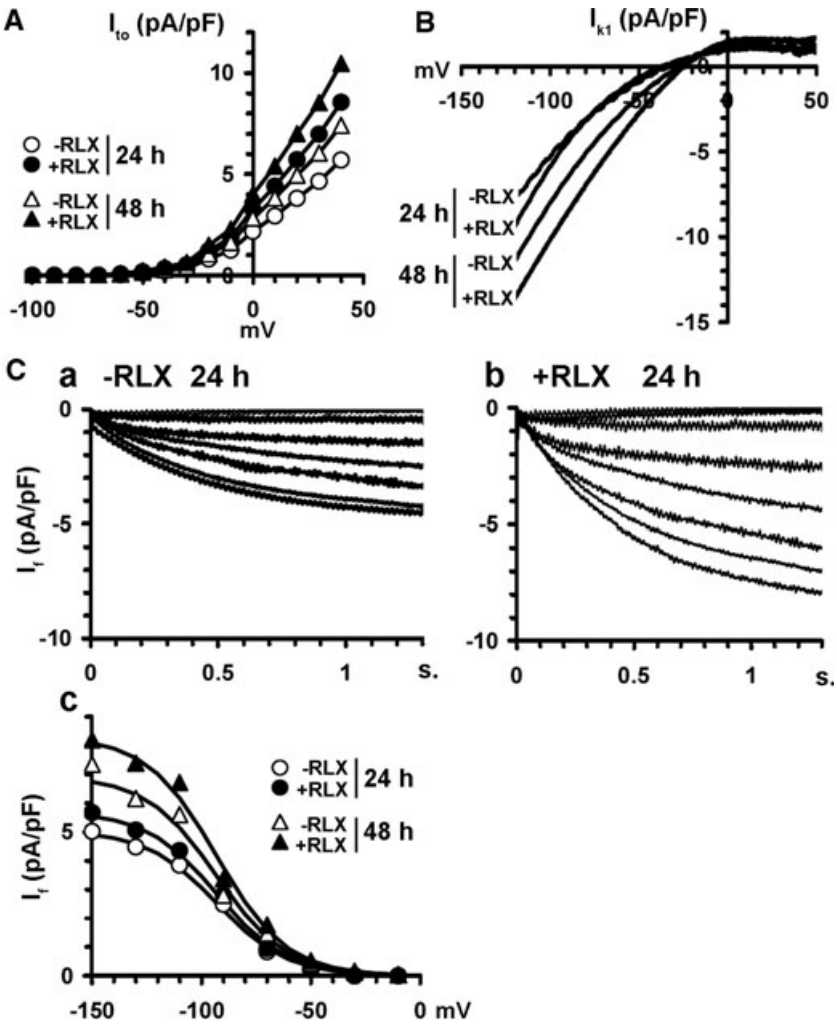

Fig. 6 Electrophysiological features of I_{to}, I_{K1} and I_f currents in the neonatal cardiomyocytes cultured for 24 and 48 hrs in the absence (control) or presence of RLX. *I–V* plots of: (**A**) outward I_{to}, and (**B**) transient inward rectifier I_{K1}, evaluated by a voltage ramp protocol. (**C**) I_f trace currents in cardiomyocytes cultured for 24 hrs in the absence (**a**) or presence of RLX (**b**) and the relevant *I–V* plots at 24 and 48 hrs (**c**). RLX increases I_{K1} size by shifting its voltage dependence towards more positive potentials and enhances the size of I_{to} and I_f. The related Boltzmann parameters and the statistical analysis are reported in Table 2. Data are mean values from 26 to 35 different cells.

(2 and 12 hrs) and a subsequent growth rate reduction in comparison with the control cultures (24 hrs), concurrently with the peak in the expression of key markers of cardiac muscle differentiation. In the longer time (48 hrs), when cells attained a more advanced degree of maturation, RLX had no more effects on cell growth. This particular behaviour of RLX is consistent with the assumption that RLX could be a physiologic regulator of cardiac cell differentiation, being able to promote growth of cardiomyocyte precursors and then support their maturation towards a functional phenotype. Of note, a similar biphasic effect of RLX on cell growth was previously reported in hormone-responsive MCF-7 breast adenocarcinoma cells, in which down-regulation of proliferation was associated with the exhibition of a more differentiated phenotype by the target cells [37,38].

The reported effects of RLX on cardiomyocyte maturation involve the activation of the typical cardiac muscle transcription factors GATA-4 and Nkx2-5, which are known to play important roles in transducing nuclear events that modulate cell lineage differentiation during the development of mature cardiomyocytes [28,29]. In addition to regulating cell growth and differentiation, there is increasing evidence that GATA-4 and Nkx2-5 also control cell survival by inducing an anti-apoptotic phenotype [39,40]. Although our study does not address this issue, it is tempting to speculate that the RLX-induced GATA-4 and Nkx2-5 up-regulation in the cardiomyocytes, besides favouring the recruitment of cardiomyocyte precursors involved in heart repair, may also contribute to increase their resistance to the hostile local environment of the diseased myocardium, thereby improving their regenerative potential. In this context, it is worth noting that exogenously administered RLX has been shown to reduce the extent of non-viable myocardium in ischaemia-reperfusion animal models [26,41] and genetic transduction of C2C12 myoblasts to secrete RLX increases their engraftment and survival in the post-infarcted hearts of swine and rats [42,43].

We also investigated the nuclear transcriptional activity downstream GATA-4 and Nkx2-5: consistent with the above findings,

we found that the expression of cardiac-specific structural genes encoding for the sarcomeric protein cTnT, the ion channel HCN4 and the gap-junction protein Cx43 was significantly increased in the RLX-treated cells as compared with the untreated ones. Moreover, the presence of RLX in the culture medium also stimulated the acquisition of typical ultrastructural signs of striated muscle differentiation, such as leptomeres and myofibrils, by the developing cells. It is well known that Cx43 forms intercellular channels which link the cytoplasmic compartments of adjacent cardiomyocytes and ensure the efficient and rapid propagation of electrical impulses [30,31] as well as the transfer of Ca^{2+} and other signals involved in the regulation of cell proliferation and differentiation [44,45]. The present observation that RLX increases Cx43 expression suggests that this may be a key mechanism of its growth- and differentiation-promoting effects. Moreover, Cx-43 participates in cellular adaptation to ischaemia [46] and its up-regulation has been found to enhance stem cell survival and engraftment in the infarcted heart [47]. These latter findings add further support to the hypothesis that RLX may render the cardiomyocyte precursors resistant to the adverse conditions of the diseased post-ischaemic heart.

The effects of RLX on cardiomyocyte maturation were further supported by the electrophysiological data. Indeed, the observed up-regulation of HCN4, a membrane channel playing a major role in cardiac automatisity [32], induced by RLX fits well with the ability of the hormone to induce the appearance of I_f, the typical HCN4-operated current. The time-course analysis of the behaviour of the myocardial cell cultures indicated that, soon after isolation and plating, the cells do not show spontaneous beating: rather, this feature appears within 12–24 hours of culture, concurrently with peak HCN4 gene transcription. This suggests that HCN4 is involved in early maturation steps of the myocardial cells, as recently reported [48]. It is conceivable that, in the longer times (which we did not explore in this study), when cardiomyocytes accomplish their maturation programme, HCN4 is only retained by the pacemaker cells and tends to disappear in the cells of the working myocardium. Of note, all the major currents involved in cardiomyocyte rhythmic electrical activity attain higher amplitudes (I_{Na}, $I_{Ca,T}$, $I_{Ca,L}$, I_f, I_{to} and I_{Kl}) and conductances (G_{Na}, $G_{Ca,T}$, $G_{Ca,L}$) upon RLX treatment, with an electrical phenotype reminiscent of that of ventricular cardiomyocytes. Moreover, the hormone increases the overall cell size, as judged by the observed increase in membrane capacitance (C_m).

It should be pointed out that the current *in vitro* culture model is composed by a vast majority of *bona fide* immature cardiomyocytes and a minority of non-muscle cells of the cardiac environment [23]. Considering that fibroblasts are also known to express RXFP1 [49], it cannot be ruled that these cells may concur, for instance by paracrine or juxtacrine mechanisms, to the observed effects of RLX on cardiomyocyte growth and maturation.

Taken together, the present findings that RLX is capable of modulating growth and promoting maturation of neonatal cardiomyocytes may be clinically relevant. In fact, evidence has been provided that RLX is released in blood in patients suffering for chronic heart failure [14,15]. This may be interpreted as an adaptive response of the heart to damage and dysfunction. Although RLX has been attributed direct inotropic effects [50], peripheral and coronary vascular actions [51,52] and marked anti-fibrotic effects in post-infarction remodelling [53] which could favourably act on the failing heart, it cannot be ruled out that this hormone could also promote the recruitment of dormant myocardial precursor cells in an attempt to repair the damaged myocardium. This hypothesis is particularly intriguing, considering that human recombinant RLX has been demonstrated to have beneficial effects in phase II clinical trials on patients suffering for congestive heart failure [19–21]. It is conceivable that, with appropriate dosage and administration protocols, RLX may be recognized a valuable therapeutic tool to enhance the ability of the myocardium to self-regenerate.

Acknowledgements

We are grateful to Dr. Manuela Balzi, Radiobiology Unit, University of Florence, Italy, for skilful help in cell cycle analysis and to Dr. Daniele Nosi, Department of Anatomy, Histology & Forensic Medicine, University of Florence, Italy, for valuable support in confocal laser scanning microscopy. This study was supported by a grant from the Italian Ministry of Education, University and Research (PRIN 2009), assigned to D. Bani.

Conflict of interest

The authors declare that they have no potential conflicts of interest to disclose.

References

1. **Hellermann JP, Jacobsen SJ, Gersh BJ, *et al.*** Heart failure after myocardial infarction: a review. *Am J Med*. 2002; **113:** 324–30.
2. **Formigli L, Zecchi-Orlandini S, Meacci E, *et al.*** Skeletal myoblasts for heart regeneration and repair: state of the art and perspectives on the mechanisms for functional cardiac benefits. *Curr Pharm Des*. 2010; 16: 915–28.
3. **Beltrami AP, Barlucchi L, Torella D, *et al.*** Adult cardiac stem cells are multipotent and support myocardial regeneration. *Cell*. 2003; 114: 763–76.
4. **Urbanek K, Rota M, Cascapera S, *et al.*** Cardiac stem cells possess growth factor-receptor systems that after activation regenerate the infarcted myocardium, improving ventricular function and long-term survival. *Circ Res*. 2005; 97: 663–73.
5. **Urbanek K, Torella D, Sheikh F, *et al.*** Myocardial regeneration by activation of multipotent cardiac stem cells in ischemic

heart failure. *Proc Natl Acad Sci USA*. 2005; 102: 8692–7.

6. **Kajstura J, Urbanek K, Rota M, *et al.*** Cardiac stem cells and myocardial disease. *J Mol Cell Cardiol*. 2008; 45: 505–13.
7. **Müller P, Beltrami AP, Cesselli D, *et al.*** Myocardial regeneration by endogenous adult progenitor cells. *J Mol Cell Cardiol*. 2005; 39: 377–87.
8. **Sherwood OD.** Relaxin's physiological roles and other diverse actions. *Endocr Rev*. 2004; 25: 205–34.
9. **Bani D.** Relaxin, a pleiotropic hormone. *Gen Pharmacol*. 1997; 28: 13–22.
10. **Dschietzig T, Stangl K.** Relaxin: a pregnancy hormone as a central player of body fluid and circulation homeostasis. *Cell Mol Life Sci*. 2002; 59: 1–13.
11. **Nistri S, Bigazzi M, Bani D.** Relaxin as a cardiovascular hormone. Physiology, pathophysiology and therapeutic promises. *Cardiovasc Hematol Agents Med Chem. (CHA-MC)* 2007; 5: 101–8.
12. **Du XJ, Bathgate RA, Samuel CS, *et al.*** Cardiovascular effects of relaxin: from basic science to clinical therapy. *Nat Rev Cardiol*. 2010; 7: 48–58.
13. **Taylor MJ, Clark CL.** Evidence for a novel source of relaxin: atrial cardiocytes. *J Endocrinol*. 1994; 143: R5–8.
14. **Dschietzig T, Richter C, Bartsch C, *et al.*** The pregnancy hormone relaxin is a player in human heart failure. *FASEB J*. 2001; 15: 2187–95.
15. **Fisher C, Berry C, Blue L, *et al.*** N-terminal pro B type natriuretic peptide, but not the new putative cardiac hormone relaxin, predicts prognosis in patients with chronic heart failure. *Heart*. 2003; 89: 879–81.
16. **Osheroff PL, Ho W.** Expression of relaxin mRNA and relaxin receptors in postnatal and adult rat brain and hearts. *J Biol Chem*. 1993; 268: 15193–9.
17. **Hsu SY, Nakabayashi K, Nishi S, *et al.*** Activation of orphan receptors by the hormone relaxin. *Science*. 2002; 295: 671–3.
18. **Kompa AR, Samuel CS, Summers RJ.** Inotropic responses to human gene 2 (B29) relaxin in a rat model of myocardial infarction (MI): effect of pertussis toxin. *Br J Pharmacol*. 2002; 137: 710–8.
19. **Dschietzig T, Teichman S, Unemori E, *et al.*** Intravenous recombinant human relaxin in compensated heart failure: a safety, tolerability, and pharmacodynamic trial. *J Card Fail*. 2009; 15: 182–90.
20. **Teerlink JR, Metra M, Felker GM, *et al.*** Relaxin for the treatment of patients with acute heart failure (Pre-RELAX-AHF): a multicentre, randomised, placebo-controlled, parallel-group, dose-finding phase IIb study. *Lancet*. 2009; 373: 1429–39.
21. **Teichman SL, Unemori EN, Dshcietzig T, *et al.*** Relaxin, a pleiomorphic vasodilator for the treatment of heart failure. *Heart Fail Rev*. 2009; 14: 321–9.
22. **Devic E, Xiang Y, Gould D, *et al.*** β-Adrenergic receptor subtype-specific signaling in cardiac myocytes from β_1 and β_2 adrenoceptor knockout mice. *Mol Pharmacol*. 2001; 60: 577–83.
23. **Formigli L, Francini F, Nistri S, *et al.*** Skeletal myoblasts overexpressing relaxin improve differentiation and communication of primary murine cardiomyocyte cell cultures. *J Mol Cell Cardiol*. 2009; 47: 335–45.
24. **Formigli L, Francini F, Tani A, *et al.*** Morphofunctional integration between skeletal myoblasts and adult cardiomyocytes in coculture is favored by direct cell-cell contacts and relaxin treatment. *Am J Physiol (Cell Physiol)*. 2005; 288: C795–804.
25. **Masini E, Bani D, Bello MG, *et al.*** Relaxin counteracts myocardial damage induced by ischemia-reperfusion in isolated guinea pig hearts: evidence for an involvement of nitric oxide. *Endocrinology*. 1997; 138: 4713–20.
26. **Perna AM, Masini E, Nistri S, *et al.*** Novel drug development opportunity for relaxin in acute myocardial infarction evidences from a swine model. *FASEB J*. 2005; 19: 1525–7.
27. **Shinagawa Y, Satoh H, Noma A.** The sustained inward current and inward rectifier K^+ current in pacemaker cells dissociated from rat sinoatrial node. *J Physiol*. 2000; 523: 593–605.
28. **Harvey RP.** NK-2 homeobox genes and heart development. *Dev Biol*. 1996; 178: 203–16.
29. **Molkentin JD.** The zinc finger-containing transcription factors GATA-4, -5, and -6. Ubiquitously expressed regulators of tissue-specific gene expression. *J Biol Chem*. 2000; 275: 38949–52.
30. **Duffy HS, Fort AG, Spray DC**. Cardiac connexins: genes to nexus. *Adv Cardiol*. 2006; 42: 1–17.
31. **Jansen JA, van Veen TA, de Bakker JM, *et al.*** Cardiac connexins and impulse propagation. *J Mol Cell Cardiol*. 2010; 48: 76–82.
32. **Baruscotti M, Barbuti A, Bucchi A.** The cardiac pacemaker current. *J Mol Cell Cardiol*. 2010; 48: 55–64.
33. **Hosokawa T, Okada T, Kobayashi T, *et al.*** Ultrastructural and immunocytochemical study of the leptomeres in the mouse cardiac muscle fibre. *Histol Histopathol*. 1994; 9: 85–94.
34. **Thomas GR, Vandlen R.** The purely chronotropic effects of relaxin in the rat isolated heart. *J Pharm Pharmacol*. 1993; 45: 927–8.
35. **Zorn-Pauly K, Schaffer P, Pelzmann B, *et al.*** L-type and T-type Ca^{2+} current in cultured ventricular guinea pig myocytes. *Physiol Res*. 2004; 53: 369–77.
36. **Boheler KR, Czyz J, Tweedie D, *et al.*** Differentiation of pluripotent embryonic stem cells into cardiomyocytes. *Circ Res*. 2002; 91: 189–201.
37. **Bani Sacchi T, Bani D, Brandi ML, *et al.*** Relaxin influences growth, differentiation and cell-cell adhesion of human breast-cancer cells in culture. *Int J Cancer*. 1994; 57: 129–34.
38. **Bani D, Masini E, Bello MG, *et al.*** Relaxin activates the L-arginine-nitric oxide pathway in human breast cancer cells. *Cancer Res*. 1995; 55: 5272–5.
39. **Toko H, Zhu W, Takimoto E, *et al.*** Csx/Nkx2-5 is required for homeostasis and survival of cardiac myocytes in the adult heart. *J Biol Chem*. 2002; 277: 24735–43.
40. **Suzuki YJ, Nagase H, Day RM, *et al.*** GATA-4 regulation of myocardial survival in the preconditioned heart. *J Mol Cell Cardiol*. 2004; 37: 1195–203.
41. **Bani D, Masini E, Bello MG, *et al.*** Relaxin protects against myocardial injury caused by ischemia and reperfusion in rat heart. *Am J Pathol*. 1998; 152: 1367–76.
42. **Formigli L, Perna AM, Meacci E, *et al.*** Paracrine effects of transplanted myoblasts and relaxin on post-infarction heart remodeling. *J Cell Mol Med*. 2007; 11: 1087–110.
43. **Bonacchi M, Nistri S, Nanni C, *et al.*** Functional and histopathological improvement of the post-infarcted rat heart upon myoblast cell grafting and relaxin therapy. *J Cell Mol Med*. 2009; 13(9B): 3437–48. Doi:10.1111/j.1582-4934.2008.00503.x.
44. **Bassel-Duby R, Olson EN**. Role of calcineurin in striated muscle: development, adaptation, and disease. *Biochem Biophys Res Commun*. 2003; 311: 1133–41.
45. **Wörsdörfer P, Maxeiner S, Markopoulos C, *et al.*** Connexin expression and functional analysis of gap junctional communication in mouse embryonic stem cells. *Stem Cells*. 2008; 26: 431–9.
46. **Lin JH, Lou N, Kang N, *et al.*** A central role of connexin 43 in hypoxic preconditioning. *J Neurosci*. 2008; 28: 681–95.

47. **Lu G, Haider HK, Jiang S, *et al.*** Sca-1+ stem cell survival and engraftment in the infarcted heart: dual role for preconditioning-induced connexin-43. *Circulation*. 2009; 119: 2587–96.
48. **Le Menuet D, Munier M, Meduri G, *et al.*** Mineralocorticoid receptor overexpression in embryonic stem cell-derived cardiomyocytes increases their beating frequency. *Cardiovasc Res*. 2010; 87: 467–75.
49. **Samuel CS, Unemori EN, Mookerjee I, *et al.*** Relaxin modulates cardiac fibroblast proliferation, differentiation, and collagen production and reverses cardiac fibrosis *in vivo*. *Endocrinology*. 2004; 145: 4125–33.
50. **Kakouris H, Eddie LW, Summers RJ.** Cardiac effects of relaxin in rats. *Lancet*. 1992; 339: 1076–8.
51. **Nistri S, Bani D.** Relaxin in vascular physiology and pathophysiology: possible implications in ischemic brain disease. *Curr Neurovasc Res*. 2005; 2: 225–34.
52. **Bani D.** Relaxin as a natural agent for vascular health. *Vasc Health Risk Manag*. 2008; 4: 515–24.
53. **Samuel CS, Cendrawan S, Gao XM, *et al.*** Relaxin remodels fibrotic healing following myocardial infarction. *Lab Invest*. 2011; 91: 675–90.